International Journal of Innovation and Applied Studies
ISSN 2028-9324 Vol. 5 No. 3 Mar. 2014, pp. 222-232

http://www.issr-journals.org/ijias/

Numerical study of natural ventilation in a channel integrated below the roof tiles of Buildings

Dalila Ababsa and Saadi Bougoul

Laboratoire de Physique Energétique Appliquée (LPEA), Faculté des Sciences, Université de Batna, Algeria

ABSTRACT: In this work, a comparative numerical study of natural convection in a channel with two types of walls was presented. This channel has two flat walls in the first case and flat wall and sinusoidal one in the second case. This type of channels is used as a thermosyphon system under the tiles of the roof of the buildings. It maximizes natural ventilation and minimizes the solar energy absorbed by the construction.
To evaluate the effectiveness of the air channel, a numerical model is developed for the studied thermosyphon using the software FLUENT.
The governing equations are solved by using the software Fluent where the SIMPLER algorithm is used for the coupling of velocity and pressure. The flow is turbulent and the turbulence is modeled by using the k-ε model.
The distributions of speeds, temperatures and mass flow induced are determined. The obtained results are in good agreement with the experimental ones.
A comparative study of the air flow in the second type of channel with sinusoidal wall was performed, it fined that it gives a flow with a high rate and the use of the corrugated surface allows us to increase the heat transfer to the fluid and the rate of mass flow without affecting the length of the channel.

KEYWORDS: Natural ventilation, temperature, speed, air channel, comparative study.

1 INTRODUCTION

The numerical and experimental studies of natural convection in inclined channels have become very interesting. This is due to the importance of the geometry in the heating and cooling of collective or individual buildings (solar chimney, Trombe wall, etc ...), in the cooling of electronic components and other applications.

The roofs are usually constructed with an air gap of 3cm located below the tiles. This thickness was recommended by the rules of buildings construction [1].

In this system, air movement which occurs naturally as a result of temperature difference caused by solar radiation can be used in heating (in winter) and cooling (in summer) of constructions.

This thermosyphon system depends on various parameters such as geometry, inclination, channel opening, solar radiation...

The increase in the exchange surface of the channel may increase the heat transfer to the fluid [2]. For this reason and in order to increase the air flow in the thermosyphon system, we propose a sinusoidal shape of the upper plate (hot plate) of the channel.

In this work, we studied the natural convection in two types of channels, the first is composed of two parallel flat plates and the second consists of a flat bottom plate and a sinusoidal top plate. The geometries are given below.

The objective of this work is to study numerically the airflow produced in both thermosyphon systems. To see the effectiveness of the two channels, a numerical model was developed. The results obtained in the form of airflow,

Corresponding Author: Dalila Ababsa (d_ababsa@hotmail.com)

temperature profiles, average coefficient of convection, and Nusselt n-umber in the case of the first channel are validated with experimental results of J. Khedari [3]. The numerical model used in the first type of channel was extended to the study of natural convection in the second one having a sinusoidal plate, this allows us to say in which channel the airflow is better.

Nomenclature

L	Channel length	m
W	Channel width	m
A	Surface of the hot plate	m^2
H	Thickness of the air gap	m
T_H	Hot temperature	K
T_b	Average temperature of the air	K
V_i	Inlet speed	$m.s^{-1}$
K	Turbulent Kinetic Energy	$m^2.s^{-2}$
U	Velocity	$m.s^{-1}$
P	Pressure	Pa
ε	Dissipation rate	$m^2.s^{-3}$
Pr	Prandtl number	
Ra	Rayleigh number	
Nu	Nusselt number	
Pr_t	Turbulent Prandtl number	
Gr	Grashauf number	
ρ	Fluid density	$kg.m^{-3}$
ν	Kinematic viscosity	$m^2.s^{-1}$
C_P	The specific heat of the fluid	$j.Kg^{-1}.K^{-1}$
β	Coefficient of thermal expansion of the fluid	K^{-1}
λ	Thermal conductivity of the fluid	$W.m^{-1}.K^{-1}$
g	Gravity	$m.s^{-2}$
ν_t	Turbulent kinematic viscosity	$m^2.s^{-1}$
b	Block	
T	Turbulent	
o	Outlet	
i	Inlet	
θ	Inclination angle of the channel	°
Mean	Mean	
Min	Minimum	
Max	Maximum	

In the literature, several numerical and experimental studies of natural and forced convection in passive systems are available. Some studies that we found, we note those of:

- The passive solar wall, which was used for heating and natural ventilation of buildings.

- The Systems of classical compounds walls. In this case, we find the numerical study validated experimentally of Jibao Shen et al. [4] and the comparative study of four types of solar walls [5].

Yanik Boutin et al [6] studied the effect of the channel width, the Rayleigh number and heat transfer coefficient on the air flow and proposed a correlation between these parameters. Another numerical study concerns the effect of heat sources distribution in the fluid flow in a channel was developed by using the Fluent software [7] and [8].

The concept of fireplace used for heating buildings is also an example of these studies and we can found the numerical study of turbulent natural convection in a vertical channel with asymmetric heating walls [9]. The objective of this study is to see the effectiveness of solar collectors installed on the walls of school buildings.

Another numerical study of solar chimney systems is that of a channel composed of two parallel walls [10].

The effect of the inclination of the solar chimney on the air flow has been studied theoretically and experimentally [11] and CFD modeling techniques [12] have been used to determine the ventilation rate in the presence of double glazing.

Another numerical study on laminar and turbulent flows induced by natural convection in channels for several Rayleigh numbers obtained for different values of the ratio of the high to the length of the channel and for different heating conditions was developed and correlation between these parameters and the Nusselt number was obtained [13]. Jongjit et Hirunlabh [14] studied the performance of a thermosyphon system similar to a solar collector integrated in the building roof. This system improves the thermal comfort of constructions.

The design of double skin walls is known as an effective method to reduce the solar gain of the building, for that an inclined open channel with a top plate heated by a lighting system is used to simulate roofs with double walls exposed to sunlight. [15].

Models of roofs inspired from the concept of walls with double skin and technical barriers to radiation have been specifically designed to reduce solar gain received by construction [16].

Experimental results have been obtained in the case of a tilted cavity heated from the top to try to reproduce the effect of solar radiation on a roof [17]. For this, the variation of the different heat flow and air flow in the cavity have been measured and interpreted.

One method of increasing the heat transfer by convection through the channels is to use corrugated surfaces. For this purpose, W. Gao [18] studied numerically the natural convection in a solar collector consisting of a flat cover and a wavy absorber.

2 STUDIED GEOMETRIES

The two geometries studied are shown in Figure.1; for each geometry the length (L) and width (w) are respectively equal to 1.36 m and 0.68 m. The height of the channel consisting of flat plates is H = 0.14 m. Channel with sinusoidal plate has a maximum height Hmax = 0.16 m and a minimum height Hmin = 0.12 m. The inclination angle is selected equal to 30°.

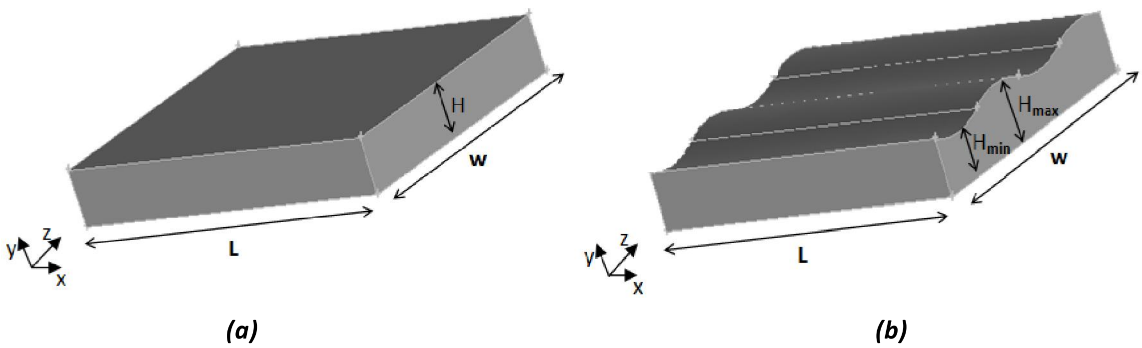

Fig. 1. Studied geometries: (a) flat plate channel, (b) channel with sinusoidal upper plate

3 THEORY

The flow within the channel is turbulent. For a steady, turbulent and compressible flow in two directions (x,y), the equations of continuity, momentum and energy can be written as [19, 20]:

$$\frac{\partial \bar{U}_i}{\partial \bar{x}_j} = 0 \tag{1}$$

$$\bar{U}_j \frac{\partial \bar{U}_i}{\partial x_j} = -\frac{1}{\rho}\frac{\partial \bar{P}}{\partial x_i} + \frac{\partial}{\partial x_j}\left[(\nu + \nu_t)\frac{\partial \bar{U}_i}{\partial x_j}\right] + g_i \beta(\bar{T} - T_0) \tag{2}$$

$$\bar{U}_j \frac{\partial \bar{T}}{\partial x_j} = \frac{\partial}{\partial x_j}\left[\left(\frac{\nu}{Pr} + \frac{\nu_t}{Pr_t}\right)\frac{\partial \bar{T}}{\partial x_j}\right] \tag{3}$$

This system of equations is obtained under the assumption that the viscous dissipation is neglected, the physical properties for the fluid are assumed constant and the gravity has a vertical effect. The Boussinesq approximation [21] is applied to the entire domain. As the flow in the channel is turbulent, the turbulence is modelled using the k-ε model.

$$\overline{U_j}\frac{\partial k}{\partial x_j} = \frac{\partial}{\partial x_j}\left[\left(\nu + \frac{\nu_t}{\sigma_k}\right)\frac{\partial k}{\partial x_j}\right] + \nu_t \frac{\partial \overline{U_i}}{\partial x_j}\left[\frac{\partial \overline{U_i}}{\partial x_j} + \frac{\partial \overline{U_j}}{\partial x_i}\right] + \frac{\beta}{\rho} g_i \frac{\nu_t}{Pr_t}\frac{\partial \overline{T}}{\partial x_j} - \varepsilon \tag{4}$$

$$\overline{U_j}\frac{\partial \varepsilon}{\partial x_j} = \frac{\partial}{\partial x_j}\left[\left(\nu + \frac{\nu_t}{\sigma_k}\right)\frac{\partial \varepsilon}{\partial x_j}\right] + \frac{C_{1\varepsilon}}{\rho}\frac{\varepsilon}{k}\nu_t \frac{\partial \overline{U_i}}{\partial x_j}\left[\frac{\partial \overline{U_i}}{\partial x_j} + \frac{\partial \overline{U_j}}{\partial x_i}\right] + \frac{C_{1\varepsilon}C_{3\varepsilon}}{\rho}\frac{\varepsilon}{k}\left[\frac{\beta}{\rho} g_i \frac{\nu_t}{Pr_t}\frac{\partial \overline{T}}{\partial x_j}\right] - C_{2\varepsilon}\frac{\varepsilon^2}{K} \tag{5}$$

For shear layers which the direction of the main flow is parallel to the gravity direction, $C_{3\varepsilon} = 1$ and for the shear layers perpendicular to gravity, $C_{3\varepsilon}$ is zero. The other constants have the following values [22]:

$C_\mu = 0.09$, $\sigma_k = 1.0$, $\sigma_\varepsilon = 1.3$, $C_{1\varepsilon} = 1.44$, $C_{2\varepsilon} = 1.92$.

In this case, the dimensionless Nusselt number Nu is a function of the Rayleigh number Ra, the Prandtl number Pr, the ratio (H/L) and the angle of inclination θ.

The fluid used is air (Pr = 0.71). The Rayleigh number Ra is defined as:

$$Ra = Gr.\,\mathrm{Pr} \tag{6}$$

Gr is a dimensionless number defined by :

$$Gr = \frac{g\beta(T_H - T_b)H^3}{\nu^2} \tag{7}$$

g is the gravity acceleration, β is the coefficient of thermal expansion, ν is the kinematic viscosity, T_H is the temperature of the hot wall and T_b is the average temperature of the air. The flow regime in the Thermosyphon is related to the values of the Rayleigh number Ra.

For large values of this number, the flow becomes turbulent. The Nusselt number Nu is a function of the height H of the thermosyphon, the Rayleigh number Ra and the angle of inclination ɵ.

$$Nu = f(Ra, H, \theta) \tag{8}$$

The Nusselt number is defined by:

$$Nu = \frac{\bar{h}H}{\lambda} \tag{9}$$

The average coefficient of convection $\bar{h}$ is given by [16]:

$$\bar{h} = \frac{Q}{A(T_H - T_b)} \tag{10}$$

Q is the convective heat flux which is expressed by:

$$Q = \dot{m}C_P(T_O - T_i) \tag{11}$$

To calculate the convective heat flux, the average temperature of the air can be used to estimate the temperature of the air at the outlet of the channel [3].

$$T_O = 2T_b - T_i \tag{12}$$

Where:

$$T_O - T_i = 2(T_b - T_i) \tag{13}$$

4 BOUNDARY CONDITIONS

The boundary conditions must be defined to solve different equations obtained. The pressure is equal to the ambient pressure at the outlet of the channel, and at the inlet temperature is equal to the ambiant temperature. For the upper and lower walls, the speed satisfies the non-slip condition and temperatures are taken equal to those chosen by J. Khedari et al [3]. This allows us to validate our model in the first type of channel. The other walls were considered adiabatic (figure.2).

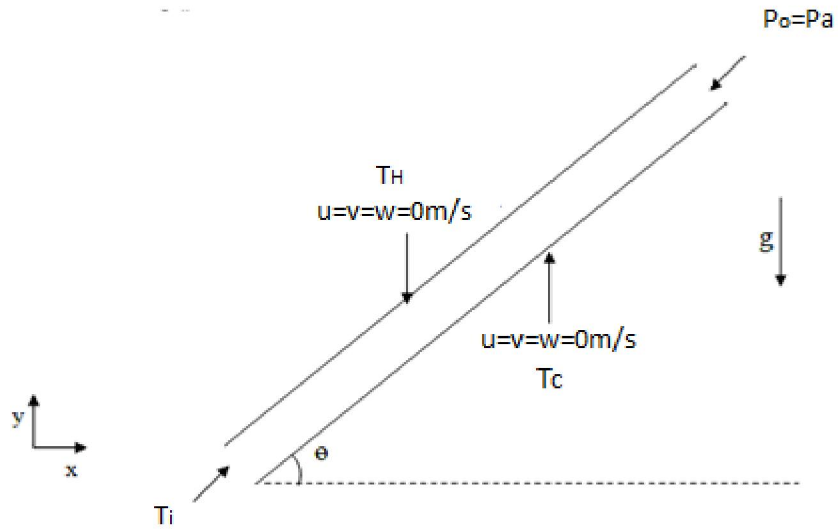

Fig. 2. boundary conditions

5 CONVERGENCE OF THE NUMERICAL RESULTS

Heat transfer and air flow which is the thermosyphon system is due to buoyancy forces (natural convection). The numerical study in these channels was performed by using the commercial computational fluid dynamics software FLUENT.

The results convergence is strongly linked to the choice of the grid, a good choice of mesh is necessary. Finer mesh can give good results, however the computation time depends on the chosen mesh, thus it needs to define the optimal between mesh and the computation time. The solution is to take a tight mesh close to the walls and slightly changing to the center of the channel (figure. 3).

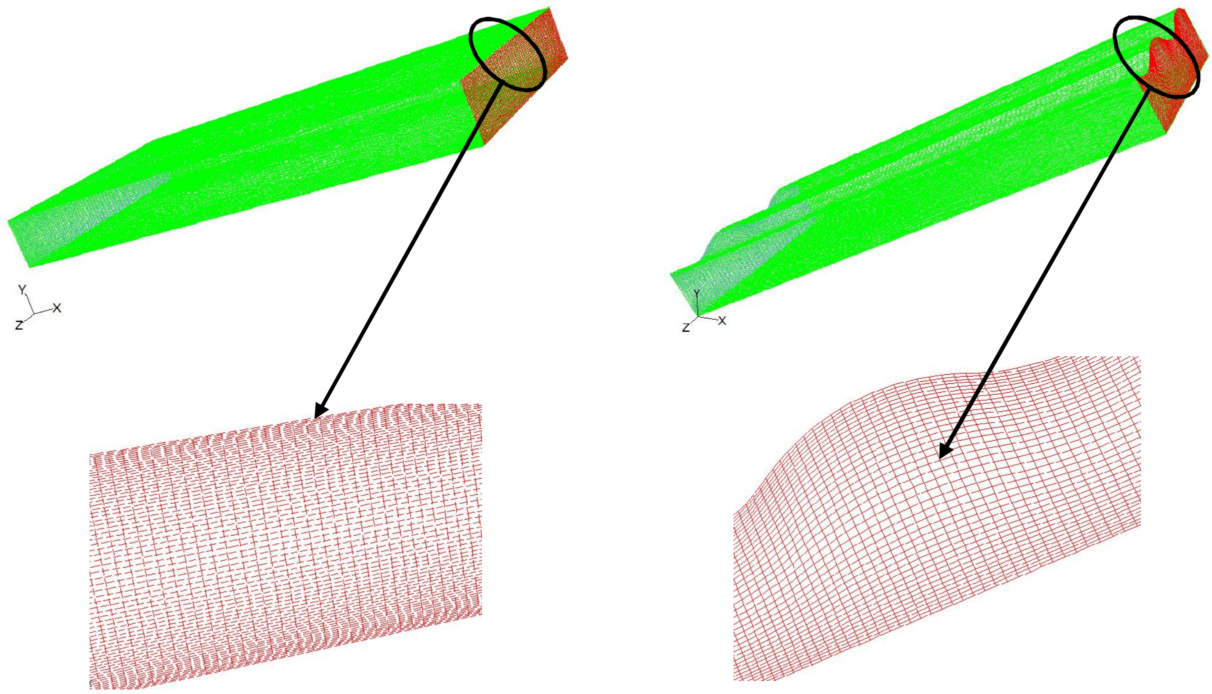

(a) *(b)*

Fig. 3. Mesh geometries studied, (a) channel flat plate, (b) channel with sinusoidal upper plate

The convergence of the numerical results is considered satisfactory if the residuals of the various parameters and the mean temperature become constant in each section.

Table 1. Tests for convergence

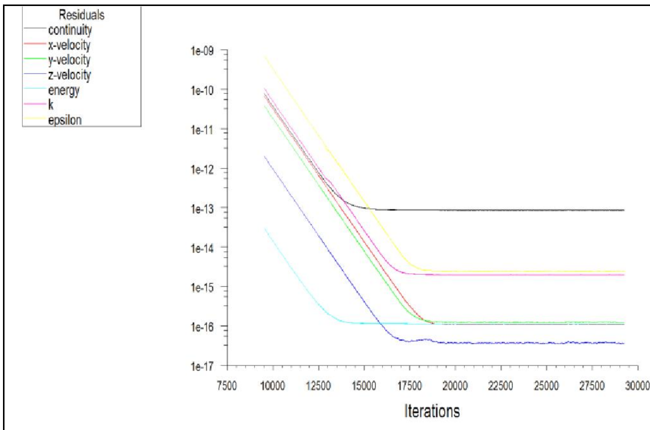

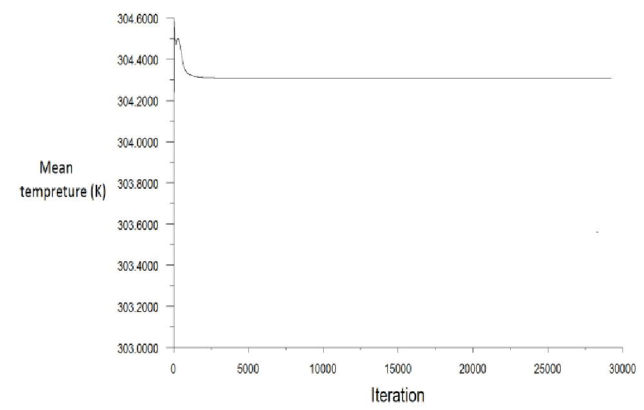

Residuals	***Convergence test of the mean temperature of the air***

6 Results and Discussion

6.1 Validation

Several cases are treated to validate our numerical model. The tests are performed by using experimental data found in the literature [3]. The inlet temperature and the hot temperature are taken as variables.

Figure 4 shows a comparison between the temperature profiles across the channel at different positions along the length, with T_H = 40.83 °C. The comparison between numerical and experimental results shows that the maximum difference is 7% for the air temperature.

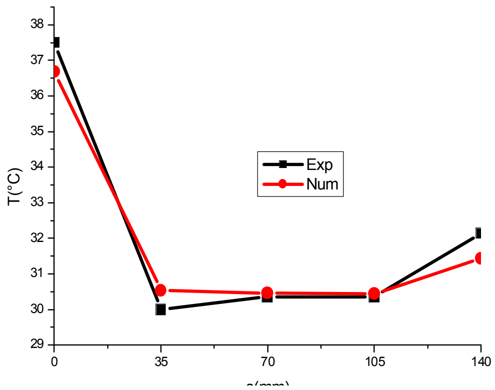

H (mm)

(a): 0.0367L

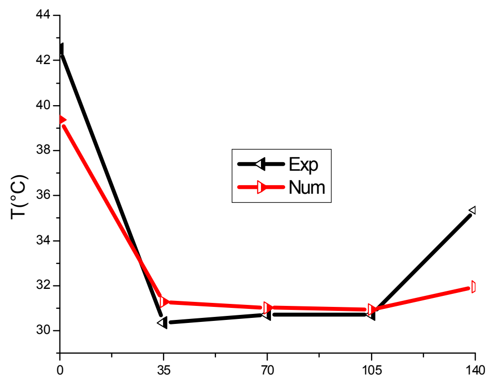

H (mm)

(b): 0.3456L

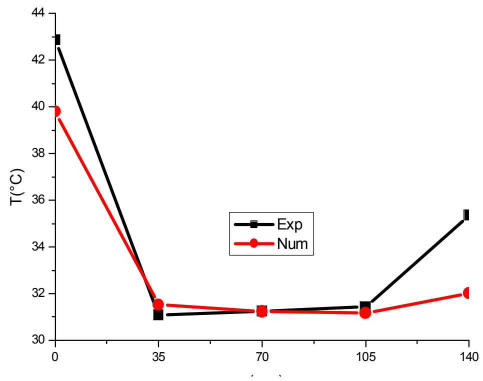

H (mm)

(c): 0.6544L

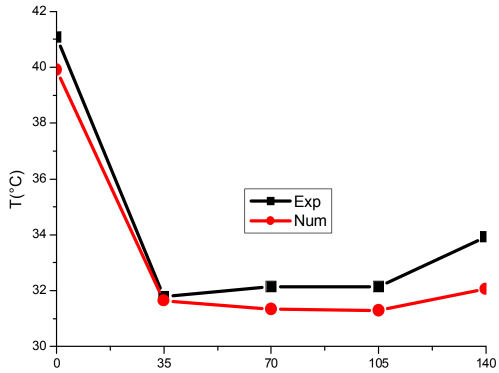

H (mm)

(d): 0.9632L

Fig. 4. Temperature profiles through the channel at different positions where Tc = 40.83 °C

The comparison between the experimental and numerical results of the values of Nusselt number (figure.5), and average convection coefficient (figure.6), shows a good agreement between the two results. The results obtained show a maximum difference of 2.6% for the Nusselt number (Nu), and an average value of 3.36% for the coefficient of heat transfer (h_{moy}). The increase of the parameter ((H/L) Ra_Hsin30°) or the Rayleigh number increases the heat transfer coefficient and consequently, the Nusselt number.

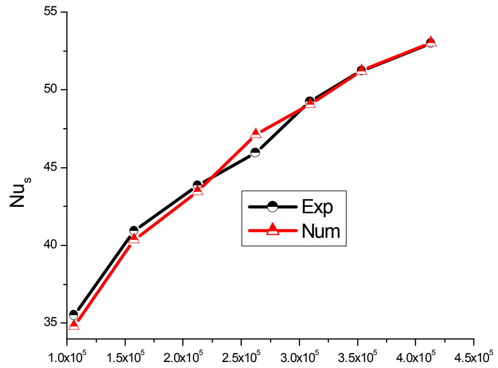

(H/L) Ra_Hsin30°)

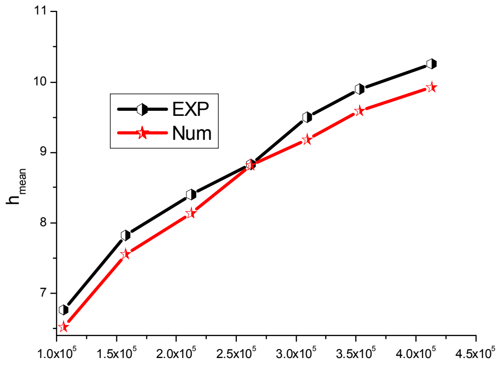

(H/L) Ra_Hsin30°)

Fig. 5. Comparison of experimental and numerical Nusselt number

Fig. 6. Comparison of experimental and numerical average coefficient of convection

A good agreement is obtained between the numerical values and the experimental values of the mass flow (Figure.7). Both results show that the mass flow increases with the increase of the parameter ((H/L) Ra_Hsin30°)).

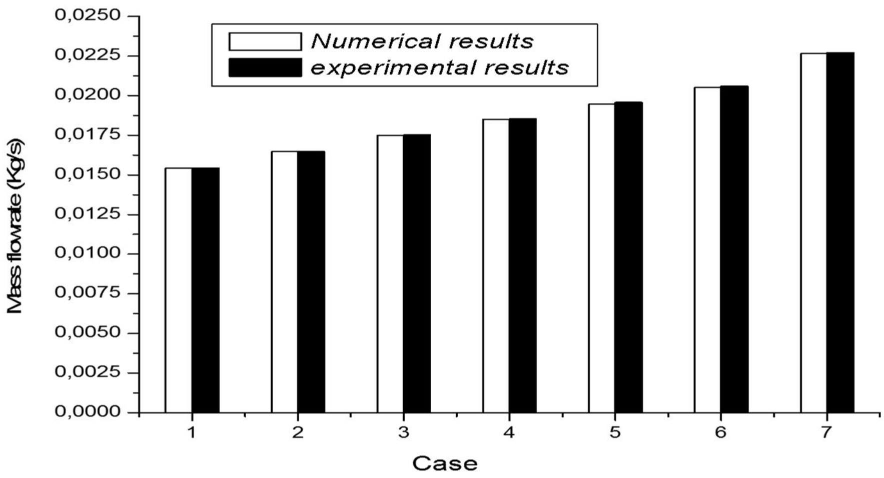

Fig. 7. ***Experimental and numerical results of the mass flow***

6.2 COMPARISON BETWEEN THE TWO TYPES OF CHANNEL

6.2.1 VELOCITY AND TEMPERATURE

The table.2 shows the velocity and temperature determined in several sections along the width of the two channels types.

The fields of temperature were highly asymmetric; this is due to the boundary conditions imposed. The high values of the velocity are near the hot plates where buoyancy forces are more dominant and on all walls the velocity satisfies the condition of non-slip.

We note that the velocity is high in the case of a sinusoidal channel then that with flat plates. For the velocity field presented in different sections of the channel, we can note that there is no recirculation of the airflow.

Table 2. Velocity and temperature field

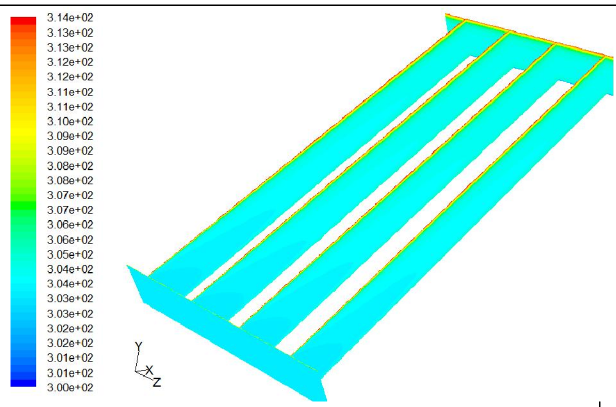	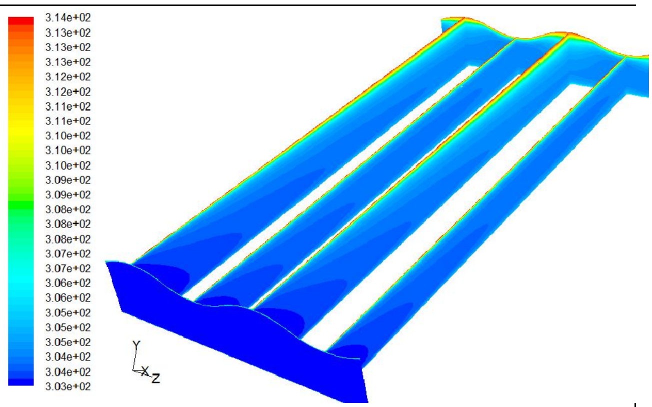
(a)	*(b)*
Field of the temperature in several sections: (a) channel flat plate, (b) channel with sinusoidal upper plate.	

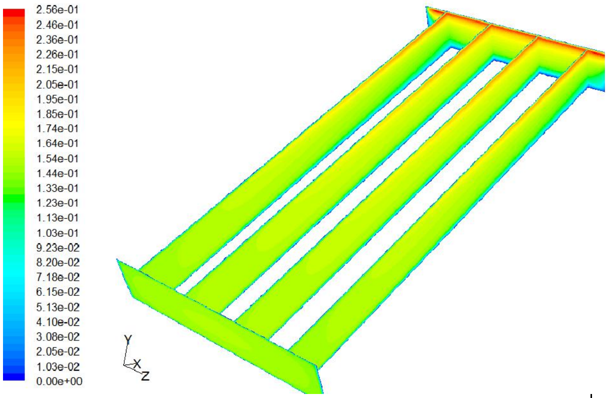	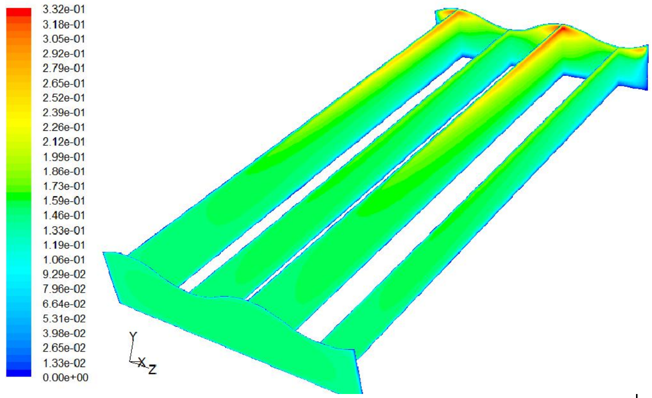
(a)	*(b)*
Velocity field in several sections: (a) channel flat plate, (b) channel with sinusoidal upper plate.	
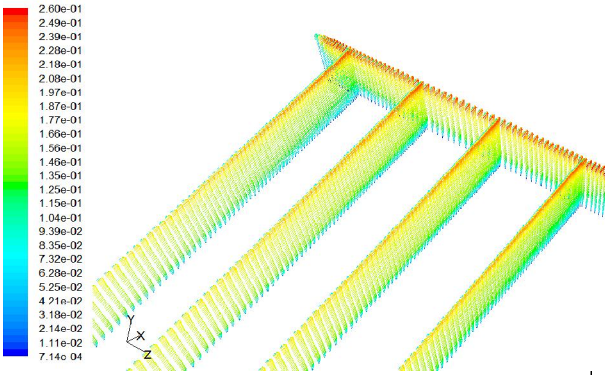	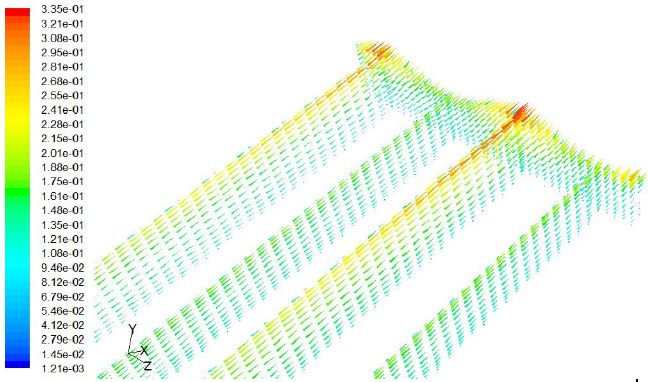
(a)	*(b)*
Velocity vectors in multiple sections: (a) channel flat plate, (b) channel with sinusoidal upper plate.	

6.2.2 MASS FLOW RATE

A comparison of the mass flow in both types of channels is shown in Figure.8. There was a significant difference in the value of the flow in both geometries. The channel with corrugated plate provides a fluid flow with a high rate. This rate is proportional to the Rayleigh number Ra.

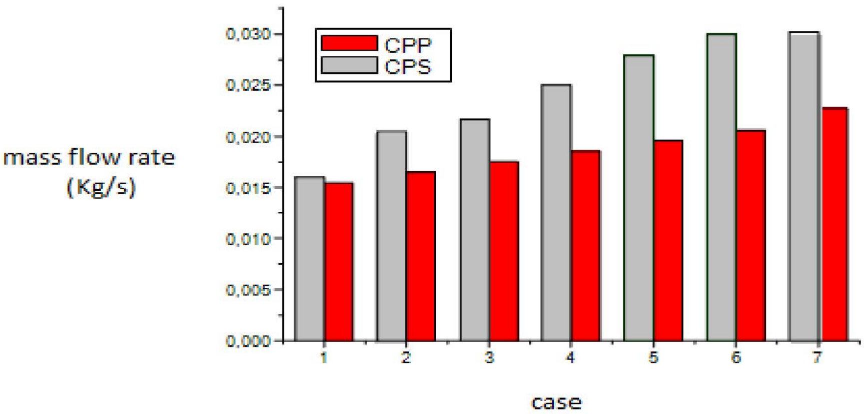

Fig. 8. Comparison of mass flow rates for both channels CPP (channel with flat plates) and CPS (channel sinusoidal plate)

6.2.3 Average convection coefficient and average Nusselt number

Figures.9 and 10 show respectively the comparison of the average convection coefficient and the average Nusselt number in both types of channels. We can see that the Nusselt number and the heat transfer coefficient have higher values in the case of channel with sinusoidal plate.

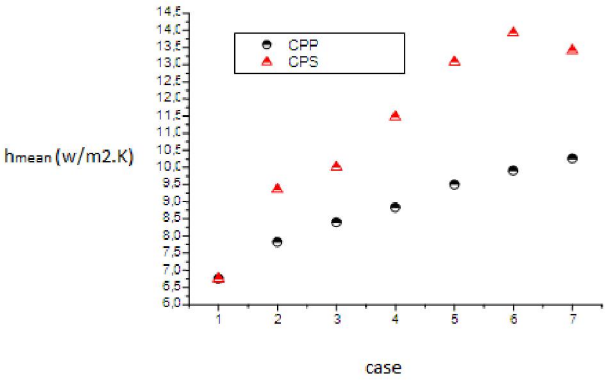

Fig. 9. Comparison of the average convection coefficient for the two types of channels

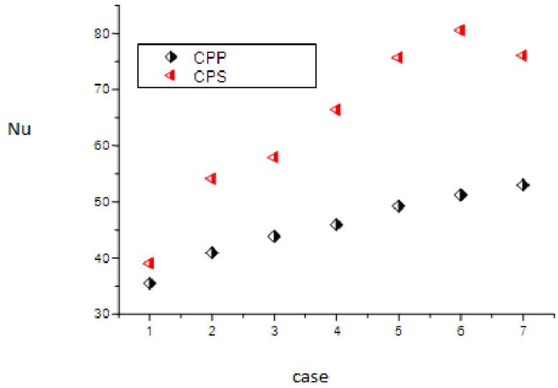

Fig. 10. Comparison of the average Nusselt number for the two types of channels

7 Conclusion

In this work the heat transfer in an inclined channel was investigated numerically by a comparison between two types of channels which can be integrated in the roof of constructions. The numerical model for the studied thermosyphon systems was developed using the software FLUENT.

The first type of channel (CPP), the temperature profiles and mass flow were validated by existing experimental results [3]. In the second channel (CPS), the velocity and temperature were presented and a comparison of the mass flow, the heat transfer coefficient and the Nusselt number for both types of channels was performed.

During this study we noticed that the temperature difference of the plates and the air temperature affects clearly the mass flow, the average coefficient of convective heat transfer, and the average Nusselt number. We can also note that the use of the corrugated surface allows us to increase the heat transfer to the fluid and the rate of mass flow without affecting the length of the channel.

References

[1] N. Chami. A. Zoughaib, “modeling natural convection in a pitched thermosyphon system present in building roofs and experimental validation using particle image velocimetry,” Energy and building, Vol. 42, pp. 1267-1274, 2010.

[2] Ho-Ming Yeh and Tong-Tshien Lin, “The effect of collector’s aspect ratio on the collector’s efficiency of flat-plate solar air,” Energy, Vol.20, pp. 1041-1047, 1995.

[3] Joseph Khedari, Patsada Yimsamerjit, Jongjit Hirunlabh, “Experimental investigation of free convection in roof solar collector,” Building and Environment, Vol.37, pp. 455-459, 2002.

[4] Jibao Shen, Stéphane Lassue, Laurent Zalewski, Dezhong Huang, “Numerical study on thermal behavior of classical or composite Trombe solar walls,” Energy and Buildings, Vol. 39, pp. 962–974, 2007.

[5] L. Zalewski, S. Lassue, B. Duthoit, M. Butez, “Study of solar walls-validating a simulation model,” Building and Environment, Vol. 37, pp. 109–121, 2002.

[6] Yanik Boutin, Louis Gosselin, “Optimal mixed convection for maximal energy recovery with vertical porous channel (solar wall),” Renewable Energy, Vol. 34, pp. 2714–2721, 2009.

[7] Jérémie Vareilles, Cristian Muresan, Stéphanie Giroux-julien, christophe menezo, ‘’étude numérique des transferts de chaleur et de masse en convection naturelle dans un canal vertical soumis a des perturbations thermiques

periodiquement reparties sur ses parois,'' 12èmes Journées Internationales de Thermique, Tanger, Maroc du 15 au 17 Novembre 2005.
[8] M. Fossa, C. Ménézo , E. Leonardi, "Experimental natural convection on vertical surfaces for building integrated photovoltaic (BIPV) applications," Experimental Thermal and Fluid Science, Vol. 32, pp.980–990, 2008.
[9] A.M. Rodrigues, A. Canha da Piedade, A. Lahellec, J.Y. Grandpeix, "Modelling natural convection in a heated vertical channel for room ventilation," Building and Environment, Vol. 35, pp. 455–469, 2000.
[10] H.F. Nouanégué, E. Bilgen, "Heat transfer by convection, conduction and radiation in solar chimney systems for ventilation of dwellings," International Journal of Heat and Fluid Flow, Vol. 30, pp. 150–157, 2009.
[11] Jyotirmay Mathur, Sanjay Mathur, Anupma, "Summer-performance of inclined roof solar chimney for natural ventilation," Energy and Buildings, Vol. 38, pp. 1156–1163, 2006.
[12] D.J. Harris, N. Helwig, "Solar chimney and building ventilation", Applied Energy, Vol. 84, pp. 135–146, 2007.
[13] B. Zamora, A.S. Kaiser, "Optimum wall-to-wall spacing in solar chimney shaped channels in natural convection by numerical investigation," Applied Thermal Engineering, Vol. 29, pp. 762–769, 2009.
[14] Jongjit Hirunlabh, Sopin Wachirapuwadon, Naris Pratinthong, Joseph Khedari, "New configurations of a roof solar collector maximizing natural ventilation," Building and Environment, Vol. 36, pp. 383–391, 2001.
[15] Chi-ming Lai, J.Y. Huang, J.S. Chiou, "Optimal spacing for double-skin roofs," Building and Environment, Vol. 43, pp. 1749–1754, 2008.
[16] Pei-Chi Chang, Che-Ming, Chi-Ming Lai, "development and preliminary evaluation of double roof prototypes incorporating RBS (radiant barrier system)," Energy and building, Vol. 40, pp. 140-147, 2008.
[17] L. Susanti, H. Homma, H. Matsumoto, Y. Suzuki, M. Shimizu, "A laboratory experiment on natural ventilation through a roof cavity for reduction of solar heat gain," Energy and building, Vol. 40, pp. 2196-2206, 2008.
[18] Wenfeng Gao, Wenxian Lin, Enrong Lu, "Numerical study on natural convection inside the channel between the flat-plate cover and sine-wave absorber of a cross-corrugated solar air heater", Energy Conversion & Management, Vol. 41, pp. 145-151, 2000.
[19] J. F. Sacadura, Initiation aux transferts thermiques, 6eme tirage, édition Technique et Documentation, 2000.
[20] Sébastien Candel, Mécanique des fluides, 2eme édition, édition Dunod, 2001.
[21] Gray DD, Giorgini A, "The validity of the Boussinesq approximation for liquids and gases," International Journal of Heat and Mass Transfer, Vol. 19, pp. 545-551, 1976.
[22] Fluent 6.3 User's Guide, Fluent Inc (2005).